S&P ARMO-System
FRCM Design Guidelines
Fiber Reinforced Cementitious Matrix

S&P

A Simpson Strong-Tie® Company

SIMPSON
Strong-Tie

Table of contents

1.   Introduction

Several different methods are available for the strengthening of existing reinforced concrete structures in building construction, civil engineering or tunnelling:

- – addition of reinforced concrete columns or beams
- – addition of steel girders
- – installation of additional steel reinforcing and concrete
- – adhesively bonded steel or FRP (Fibre Reinforced Polymer)
- – etc.

S&P is a global leader in developing, manufacturing and distributing FRP reinforcements. S&P's FRP systems can be affixed to existing structural elements as sheets, mats or prefabricated laminates using certified adhesives. Various national norms and design guidelines exist regarding adhesively bonded reinforcements made of fibre-reinforced plastics:

- • SIA 166 Norm for adhesive reinforcing (CH)
- • General building authority approval Z-36.12-68/70 (Germany)
- • Recommendations for FRP reinforcements:
  - – ACI 440 (USA)
  - – TR 55 (UK)
  - – CUR 91 (NL)
  - – CNR-DT 200/2004 (IT)
  - – etc.

Building authority approvals for S&P FRP reinforcement systems have been granted in other countries like France or Korea as well. FRP reinforcement systems are state of the art worldwide and have established themselves as a cost-effective and durable method for subsequent strengthening over the past 20 years.

> **While the stress limit is the determining factor when dimensioning reinforcement steel in reinforced concrete, strain limit is generally applied for FRP. The permissible limit strain depends on the type of load (flexural tension, shear or axial reinforcement) and the FRP system being used.**

The limit strains are defined differently in the various FRP codes, guidelines, or national technical approvals depending on the safety concept. The following limit strains are currently used in detailed design depending on the applied norms or guidelines:

Increase of stiffness using C-FRP (Carbon reinforcement)

Flexural tensile reinforcement
CFRP-laminates (surface application)	~ 0.6 – 0.8 %
Carbon Sheets (surface application)	~ 0.8 – 1.0 %
CFRP-laminates (slot-applied)	~ 0.8 – 1.0 %
CFRP-laminates (externally prestressed at 6 ‰)	~ 1.0 – 1.2 %

Axial compression column reinforcement
Carbon sheets(wrapping)	~ 0.4 %

Shear reinforcement
Carbon sheets (wrapping)	~ 0.2 – 0.4 %

Improvement of ductility using G- / A-FRP

Glass sheets (wrapping)	3 – 4 %
Aramid sheets (wrapping)	2 – 3 %

S&P has developed a new FRCM (Fiber Reinforced Cementitious Matrix) strengthening system called *S&P ARMO-System* and applied for a patent in 2009/2010. S&P proposes a design method for the FRCM strengthening system based on currently valid FRP design concepts. For the *S&P ARMO-System*, carbon mesh is rolled out on site, laid out and grouted using a reactive mineral spray mortar. For FRCM system (Fibre-Reinforced Cementitious Matrix) guidelines were introduced in the USA in October 2011 (AC 434). As the *S&P ARMO-mesh* is treated with amorphous silica and the mortar includes a reactive component, calcium silica hydrate grows from the mortar into the carbon filaments of the S&P reinforcing (Figure 1 / 2). This results in a shear-resistant interlocking and anchoring of the *S&P ARMO-mesh* with the spray mortar.
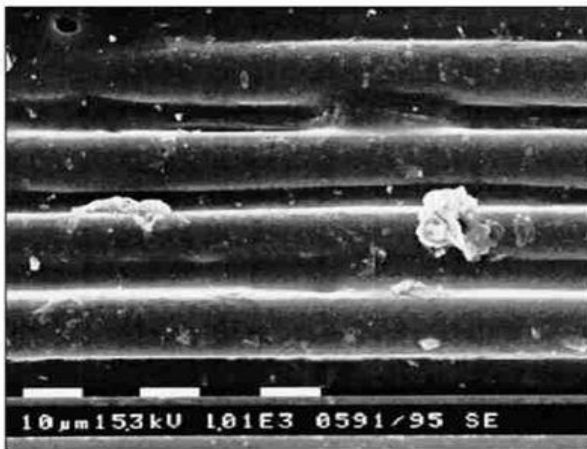

Figure 1: S&P ARMO-mesh with traditional spray mortar   Figure 2: S&P ARMO-mesh in ARMO-crete
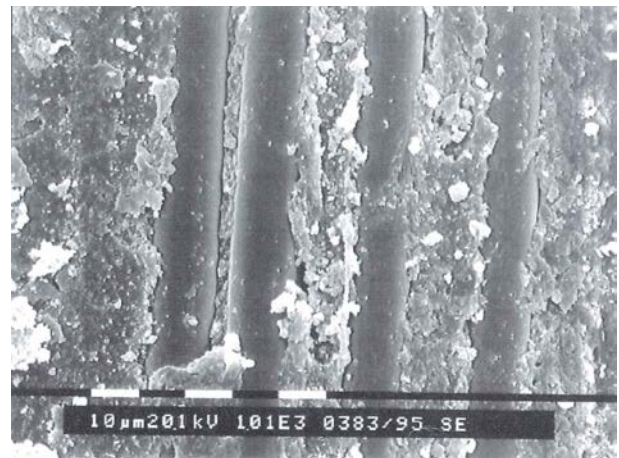
S&P offers various spray mortars with reactive components for different applications:
- *S&P ARMO-crete d*   dry-mix spray mortar (various grains, admixtures and cements)
- *S&P ARMO-crete w*   wet-mix spray mortar
- *S&P ARMO-mur*   plaster for various applications

In addition, the *S&P ARMO-mesh's* coating is tempered. This tempering creates an oxygen barrier at high temperature. The carbon fibre bundles are therefore shielded from oxidation in case of fire.

2.   Comparison of FRP / FRCM Systems

FRP reinforcements are applied to concrete, wood, or other materials using shear-resistant epoxy resin adhesives. The tensile modulus of elasticity of epoxy adhesives is roughly four times smaller than the tensile elastic modulus of concrete. Thus the thickness of the adhesive layer of CFRP laminates is limited to 3 – 5 mm. For thicker layers, the load transfer from the CFRP strip into the concrete structure cannot be ensured. When using FRP systems the unevenness of the underlying surfaces must be re-profiled using a system-approved mortar before the adhesive is applied.

Usually, re-profiling mortars are applied on an epoxy resin basis (PC, PCC). With the S&P FRCM System however, the S&P ARMO-spray mortar matrix is optimally attuned to concrete bearing surface as a material. The tensile elastic modulus of mineral spray mortar is comparable to that of concrete. Mineral spray mortar has a high pH-value and is permeable to water vapour. Re-profiling and application of the carbon reinforcing is performed in a single operation.

> **Re-profiling is unnecessary when using the S&P FRCM System. Re-profiling occurs during the application of the spray mortar layer in a single operation.**

In order to ensure the evenness of the *S&P ARMO-mesh* S&P application guidelines must be followed. The first spray mortar layer is leveled out, so that the carbon reinforcement can be worked into it. The *S&P ARMO-mesh* can be fixed using several possible methods:

- If *S&P ARMO-crete w* (wet) spray mortar or *S&P ARMO-mur* plaster mortar is used, then the *S&P ARMO-mesh* can be worked into the leveled out mortar layer without any special fastening measures.
- If *S&P ARMO-crete d* (dry) mortar is used, the following three possible fastening systems are available:
  - Provisional fixation of the *S&P ARMO-mesh* and covering of the reinforcement by spraying *S&P ARMO-crete d* onto it
  - S&P adhesive clamps (using the clamps allows fixation of the reinforcing on somewhat hardened spray mortar)
  - S&P dowels (for fixation on fully hardened bearing surfaces)

Table 1 shows a comparison between FRP and FRCM systems.

	FRP System Carbon within Epoxy Matrix	S&P FRCM System Carbon within Mineral Matrix
Moisture of structural surface	< 4% residual moisture	Earth-dry structural surface
Surface Conditioning	slight roughening (grinding or sand blasting)	Deep roughening (3 – 5 mm) (sand blasting or water jetting)
Re-profiling works	great effort for levelling / re-profiling	No additional effort
Application	Easy / convenient	Great installation effort (rendering, covering)
Building physics	Additional verification necessary FRP acts as a local vapour barrier	No additional verification necessary ARMO-System is a mineral system and permeable to vapour
Corrosion Protection of Interior Reinforcing	Additional works necessary – Corrosion protection of steel rebars – Impregnation or thin coating between FRP strengthening layers	pH-Value of 12 for *S&P ARMO-System* No additional works are necessary. *S&P ARMO-System* offers alkali protection for interior reinforcing.
Fire Safety	Residual safety in case of fire must be verified and if necessary fire safety measures must be applied.	If the *S&P ARMO-mesh* is covered 2 cm with S&P ARMO-crete, normally a fire resistance according ETS curve of R120 is given

Table 1: Comparison of FRP and FRCM Strengthening Systems

3.   Anchoring and Overlapping of *S&P ARMO-mesh*

Transferring loads from the steel reinforcement into the concrete is achieved through the use of ribbed reinforcing bars which enhance the bond between the two materials. For ribbed reinforcing the following simple rule applies:

"Lap length for reinforcing bars = 40 - 60 x Ø reinforcing bar"

The tensile strength of carbon fibres is seven to eight times higher than that of reinforcing steel. Also, carbon-fibre bundles do not possess any surface texture. *S&P ARMO-mesh* layers are also not spot welded as are reinforcing steel meshes. In order to improve the anchoring of the *S&P ARMO-mesh* in spray mortar, a special coating of the mesh surface was developed by S&P. The coating consists of an aqueous polymer that is tempered with amorphous silicate. A reactive component is included in the spray mortar *S&P ARMO-crete* or *S&P ARMO-mur*, respectively. The necessary anchorage length of *S&P ARMO-mesh L500* was verified in-house by S&P [P11] as well as externally at FH Fribourg [P23] using pull-out tests on double concrete specimens. Figures 3 / 4 / 5 show the test arrangement used in the in-house experiments.

3.1   S&P In-house Tests

Figure 3: Double concrete specimen before testing

Figure 4: Application of spray mortar and *S&P ARMO-mesh L500*

Figure 5: Test Specimen after pull-out test

A total of 12 specimens were tested while varying the following parameters:

− Anchorage length (10 or 30 cm)
− Traditional spray mortar (no reactive component)
− *S&P ARMO-crete w* spray mortar (with reactive component)
− Application of one, respectively two layers of *S&P ARMO-mesh L500*

Graph 1 shows the results of the pull-out tests. The *S&P ARMO-mesh L500* was always pulled out from its anchorage.
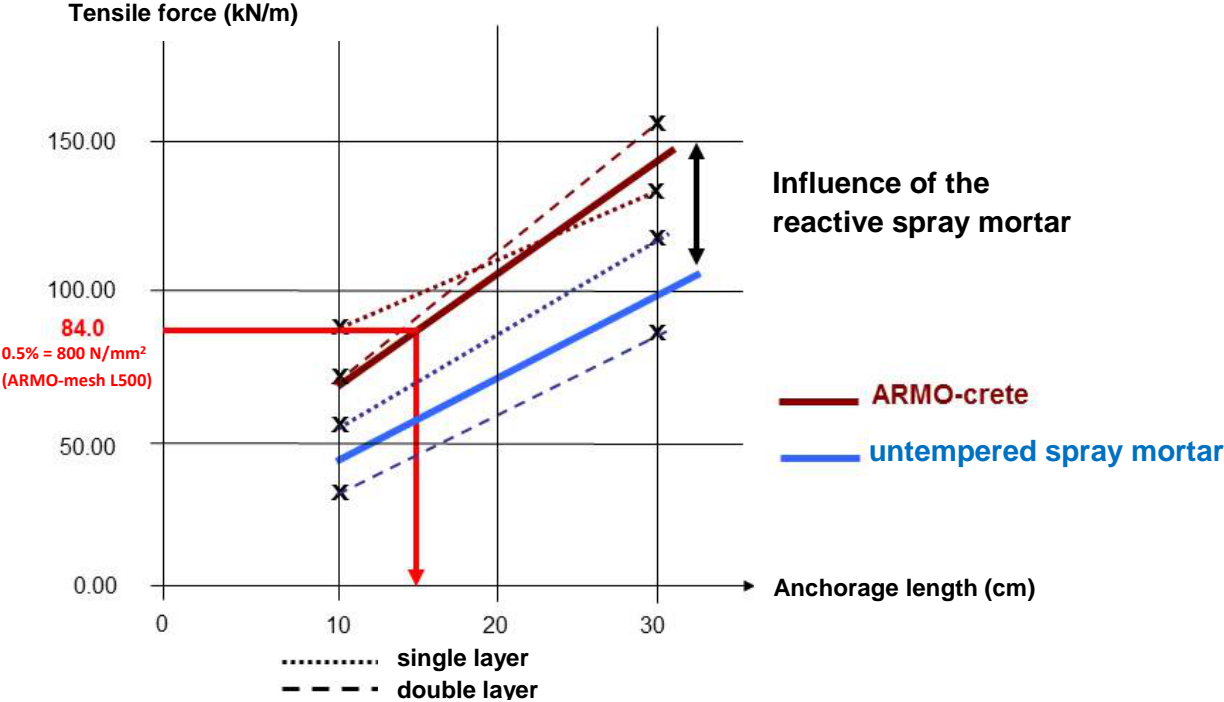
Graph 1: Results of the pull-out tests

The influence of the reactive component is clearly visible in Graph 1. If *S&P ARMO-mesh L500* is used under flexural tension in a design situation with 5 ‰ of limit strain, a force of 84 kN/m must be anchored (refer to Table 2). This corresponds to a tensile stress of 800 N/mm^2 in the *S&P ARMO-mesh L500*.

> **The reactive component of the spray mortar reduces the anchorage length by approx. 30 %.**

The S&P in-house tests were corroborated independently by FH Fribourg/CH.

3.2   Tests at FH Fribourg/CH (School of Engineering and Architecture)

The *S&P ARMO-Systems* was applied to masonry and anchored at the top and bottom on a concrete surface of 30 cm length. The *S&P ARMO-mesh* was pulled out of its anchorage during the test. The stresses in the *S&P ARMO-mesh* during the pull-out tests are shown in Graph 2 / Figure 6 as well as Table 2.

**Anchorage length
in concrete L = 30 cm**

Elevation   Section
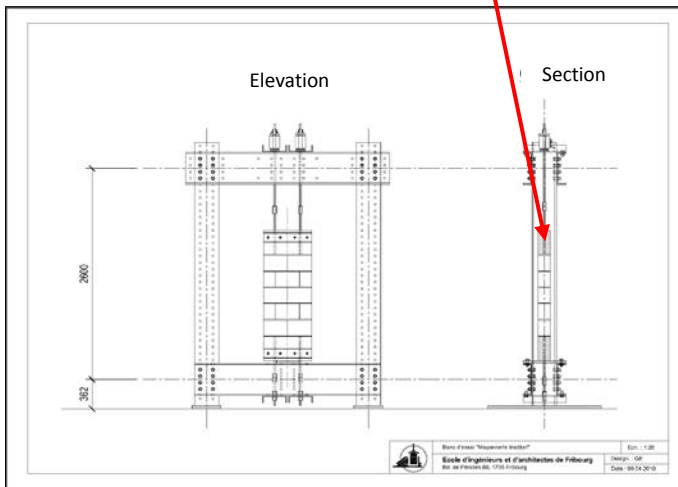
Graph 2 / Figure 6: Test Arrangement at FH Fribourg/CH

	L200	L500
Stress in ARMO-mesh *(pull-out test)*	1304 N/mm²	943 N/mm²
Flexural tensile stress in ARMO-mesh *(S&P recommendation according to technical data sheet)*	~ 800 N/mm² (flexural) ~ 650 N/mm² (axial)	

Table 2: Results of tests performed at FH Fribourg/CH

> **For the *S&P ARMO-mesh L500* at design state, the minimum anchor length should not be less than 300 mm.**

4.   S&P Alu Anchorage Element

When strengthening flexural elements with *S&P ARMO-mesh* there may be cases where anchoring the reinforcement behind the point of zero moment is not possible due to the lack of sufficient development length (Graph 3).
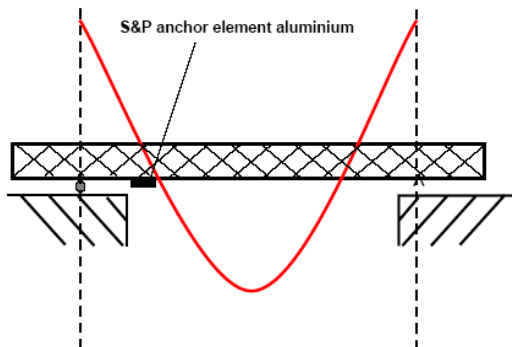
Graph 3: Anchorage behind point of zero moment   *Graph 4: S&P Alu Anchorage Element*
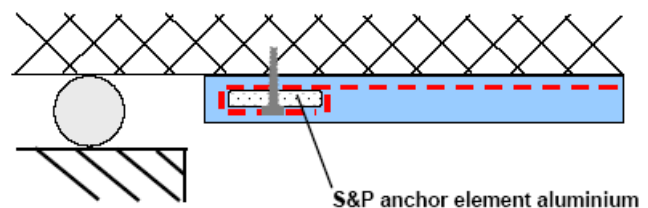
In these circumstances, the remaining force in the *S&P ARMO-mesh* is anchored behind the point of zero moment using the S&P anchorage element made of aluminium (Graph 4).

> **The load transfer into the structural surface occurs primarily through the front of the anchorage element and thus through the connecting joint between spray mortar and structural surface. The dowel of the S&P Alu anchorage element is designed only for the necessary contact pressure in order to fasten the anchorage element within the mortar.**

The effectiveness of the S&P Alu anchorage element was proven using plate bending tests at the VSH Hagerbach test tunnel [P 10 / P 20]. Graph 5 shows the VSH test arrangement. A 60 cm span was chosen for the plate bending test. The anchorage length (length beyond load transfer) on both sides is thus only 50% of 60 = 30 cm.
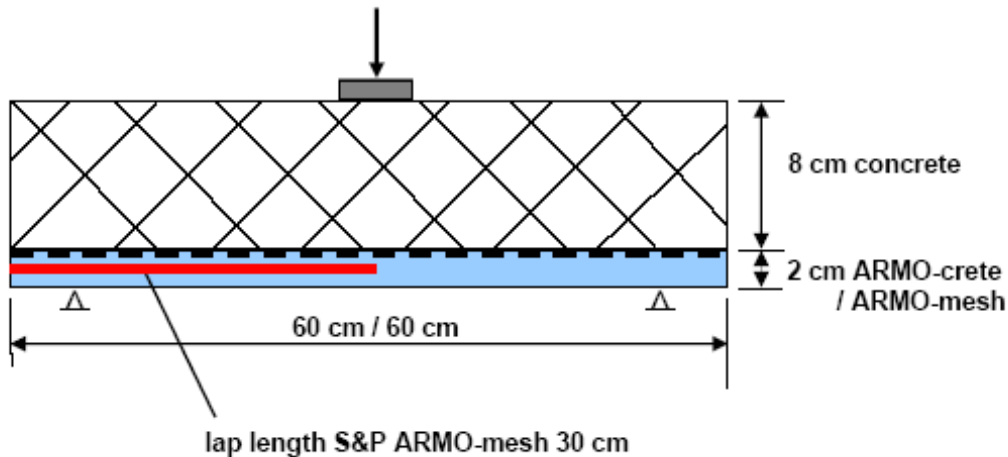
Graph 5: VSH plate bending test arrangement

At the VSH, three tests with *S&P ARMO-mesh L500* were performed with and without end anchorage. *S&P ARMO-crete d* (4 mm grain) spray mortar was used in the tests. Graph 6 and 7 show the VSH test results (average value from three test specimens each).
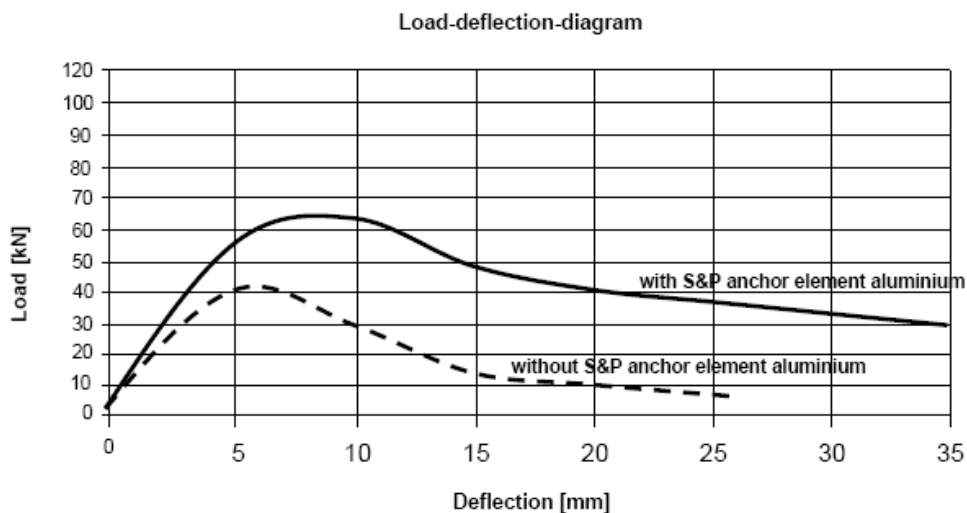
Graph 6: Load-deflection diagram for test specimens with and without anchoring
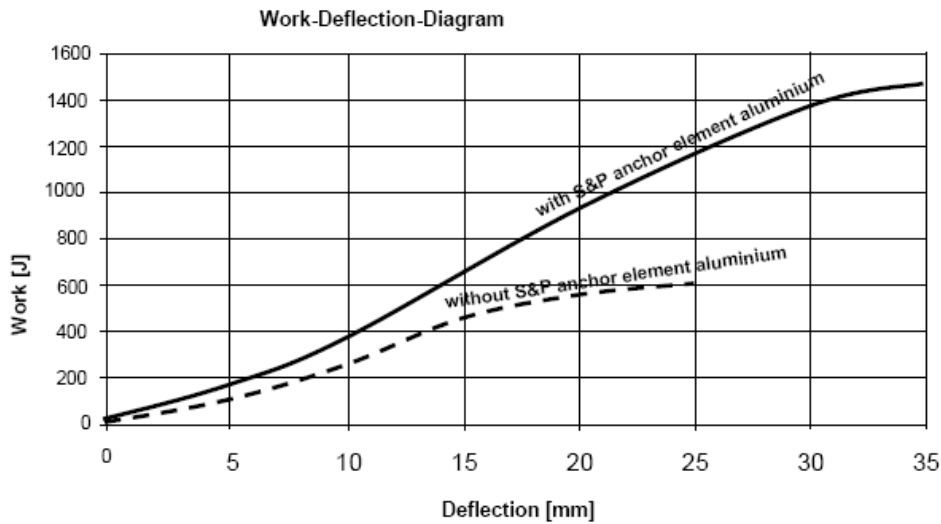
Graph 7: Work-deflection diagram for test specimens with and without anchoring

Results: 626 J   Work capacity without S&P end anchorage Alu
           1139 J **(+ 82 %)**   Work capacity with S&P end anchorage Alu

> **In the plate bending test (Figures 7 / 8) without anchoring of the *S&P ARMO-mesh* the Carbon bundles were pulled into the test specimen. The S&P Alu End Anchorage was able to prevent this. Failure there occurred because of the spray mortar delaminating. The end anchorage also increased the work capacity (J) by 82 %.**

Figure 7: VSH test arrangement

Figure 8: VSH test specimen at failure

5. Flexural Tension Strengthening using S&P FRCM System FH Fribourg/CH

The structural design for the *S&P ARMO-System* is performed following currently valid FRP design guidelines, codes or technical approvals. At the FH Fribourg basic experiments [P 15, Pub. 10] were performed on the *S&P ARMO-System* based on previous test series performed on the *S&P FRP-Systems*.

Figure 9 and Graph 8 show the test arrangement at FH Fribourg/CH.

Figure 9: Test arrangement at FH Fribourg/CH
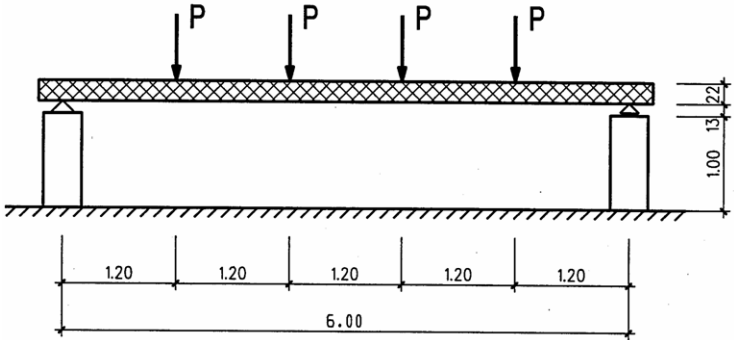
Graph 8: Test arrangement at FH Fribourg/CH

Dimension of RC slab: *Interior reinforcement:*
Thickness 22 cm   Total length 6.3 m   *longitudinal 6 Ø 12 (S 500)*
Width 85 cm   Span 6.0 m   *lateral Ø 8 S = 150 (S 500)*

An unreinforced reference slab (D0) was compared to a single layer (slab D1) and double layer (slab D2) ARMO strengthening using *S&P ARMO-mesh L500*. As spray mortar the cementitious wet spray mortar *S&P ARMO-crete w* (with reactive component) was used (Figure 10).

Figure 10: Application of the S&P FRCM System

5.1   Results of the FH Fribourg/CH Load Tests [P15]
5.1.1   Structural Behaviour at the Serviceability State

Uncracked State

As the load-deflection curves (Graph 9) present, the test specimens show only small differences in structural behavior at the uncracked state I. The main differences lie in the flexural stiffness and cracking load (Table 3).

Reference Slab D0 is significantly more flexible than the reinforced slabs; this is certainly due to the larger moment of inertia of the reinforced slabs, although this cannot be the only explanation. The flexural stiffness of the reference slab is lower due to other reasons; they can be explained with elastic calculations but will not be elaborated upon further there. The difference correspond, however, roughly to the difference in slab thickness including spray mortar strengthening.

The flexural tensile stresses deducted from the cracking moments (while considering the dead loads of the slabs and the test arrangement) correspond roughly to the flexural tensile strengths. Thus, the uncracked behavior does not show any significant surprises.

Test	δ [mm] at $Qtot = 4$ kN		In [-]	Cracking moment [kNm]	Flexural Stress [N/mm²]
D0	1.27	100%	100%	25.3	3.7
D1	0.69	55%	110%	26.6	3.4
D2	0.62	49%	115%	27.3	3.3

Table 3: Characteristic values at the uncracked state
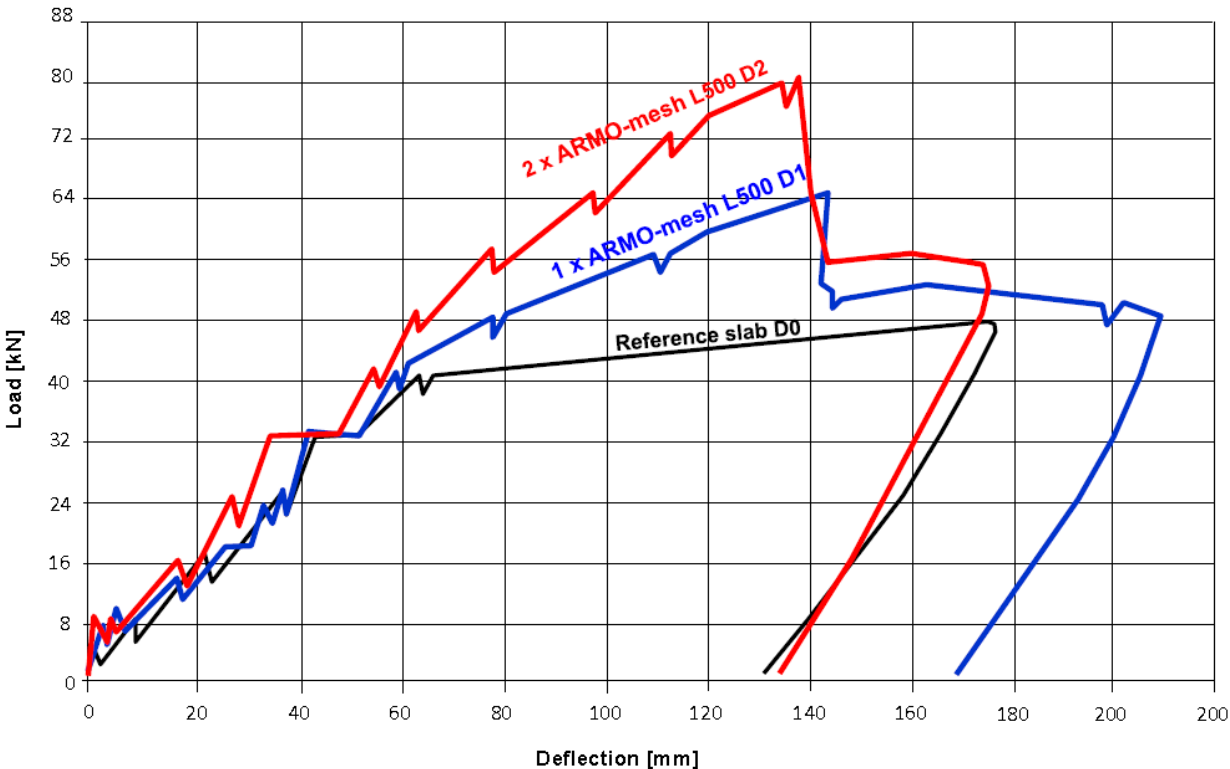
Graph 9: Deflection curves under total load at mid-span for all test specimens

Stiffnesses at the Cracked State

The Reference Slab D0 exhibits a 5.40 times lower bending stiffness at the cracked state II than at the uncracked state I (Tables 4 and 5 for the deflection increase from 8 kN to 16 kN). For the load increase from 8 kN to 24 kN and 32 kN the bending stiffness is reduced by a factor of 5.00 and 4.88, respectively; the stiffness reduction is thus slightly lower as loading increases. For the degree of reinforcement used, the theoretical stiffness reduction when calculated according to empirically based recommendations of Swiss Norm SIA 262 (Expression [N1], Eq. 102) is 5.6, which confirms the order of magnitude. The loading and unloading cycles result in an additional stiffness reduction of about 14%.

The behavior of Test Slab D1 approaches that of the reference slab as crack formation increases. The stiffness reduction at the cracked state for Girders D0 and D1 is roughly comparable to the difference in stiffness at the uncracked state. The flexural stiffness at the cracked state is reduced for D1 by a factor of 10.86 down from the uncracked stiffness (with loads increasing from 8 kN to 16kN). For the load increase from 8 kN to 24 kN and 32 kN the bending stiffness is reduced by a factor of 10.07 and 9.39, respectively; the stiffness reduction thus decreases more markedly as loading increases than it does for Reference Slab D0. The loading and unloading cycles result in an additional stiffness reduction of about 17%.

δ [mm] at $Q_{tot} =$										
Test	8 kN		16 kN		24 kN		32 kN (before load cycles)		32 kN (after load cycles)	
D0	8.98	100%	22.66	252%	34.31	382%	46.03	513%	52.32	583%
D1	5.81	65%	20.89	233%	33.60	374%	44.67	498%	52.39	583%
D2	4.41	49%	16.89	188%	28.51	317%	39.38	438%	48.02	535%

Table 4: Characteristic stiffness values at the cracked state

Test Slab D2 generally exhibits somewhat stiffer behavior than the other two test specimens. The stiffness reduction at the cracked state for Slabs D0 and D2 is equivalent to the difference in stiffness at the uncracked state. The flexural bending stiffness when Slab D2 is cracked is 10.09 times lower than its stiffness when uncracked (for a deflection increase from 8 kN to 16 kN); for a load increase from 8 kN to 24 kN and 32 kN the bending stiffness is reduced by factors of 9.72 and 9.40, respectively. The stiffness reduction is analogous to that of the reference slab, but at a much higher loading level. The loading and unloading cycles result in a further stiffness reduction of 22 %.

Test Slab D2 clearly shows the influence of the stronger *S&P ARMO-mesh* strengthening as it exhibits a stiffer behavior from the very beginning of cracking; in comparison to Slab D1 the deflections at the same load and comparable modulus of elasticity of the concrete are much smaller. In comparison to the reference slab, the increased stiffness of the tensile zone can be read very easily. The much more strongly curved increase seen for Slab D1 shows that for this test specimen, the carbon mesh reinforcing only increasingly takes on loading when the crack formation is much further along.

Working Loads for Deflection Limits

Table 5 provides a comparison of possible loads for common deflection limits. The deflections measured in the tests do not take the structural behavior under repeated loading into consideration; this influence could e.g. be estimated based on the loss of stiffness due to the load cycles. The comparison of the achieved working loads for a given deflection limit shows that carbon mesh-reinforced spray mortar layers are more effective for low levels of loading than for higher ones.

	Q_{exp} [kN]						$(Q_u/Q)_{exp}$					
	for a L/300 deflection at mid-span of											
Test	L/500		L/350		L/300		L/500		L/350		L/300	
D0	9.40	100%	12.75	100%	14.34	100%	5.02	100%	3.70	100%	3.29	100%
D1	11.48	122%	13.16	103%	15.40	107%	5.56	111%	4.85	131%	4.15	126%
D2	13.00	138%	16.00	125%	17.47	122%	6.16	123%	5.00	135%	4.58	139%

Table 5: Working loads for set deflection limits

For Test D1 the strengthening effect becomes virtually nonexistent as working loads increase; for Test D2 a reserve remains even at higher load levels. This would indicate that for lower loads the stiffness increase is mainly based on the spray mortar layer itself and less on the carbon mesh reinforcing.

If crack widths are used as serviceability criteria, then at best, higher loads might be admissible than those listed in Table 5.

Crack Widths

Table 6 lists the highest crack widths measured at the various load levels. For the lower load levels, no significant influence of the spray mortar layers or carbon mesh reinforcements can be seen. On the contrary, with increasing thickness of the spray mortar layer, the crack widths also increase. Taking into consideration the possible accuracy of the crack width measurements, an influence of the reinforcement on the crack width can only be seen beginning at a load level of 24 kN.

The measured crack widths also show that the stiffness of the carbon mesh is only activated after a certain elongation. The larger crack widths at the lower load levels are due to the increased concrete cover, as seen from the reinforcing steel; for the same steel strain, a larger crack width is to be expected as concrete cove depths increase. If a maximum crack width of 0.3 mm is defined as a serviceability criterion then for the tested slabs a total working load of 24 kN would be acceptable irrespective of the reinforcement. As this value is independent of the reinforcement applied, this is another indication of the reinforcement only being activated after the common working load levels have been reached.

Test	8 kN	16 kN	24 kN	32 kN	40 kN	48 kN	56 kN	64 kN	72 kN
D0	0.10	0.20	0.30	0.40	0.50	--	--	--	--
D1	0.20	0.25	0.30	0.35	0.60	0.80	1.10	--	--
D2	0.25	0.30	0.30	0.45	0.55	0.60	0.65	0.75	1.00

Table 6: Largest measured crack widths [mm]

Decisiveness of the Serviceability

For the dimensioning of bearing structures according to [N2], proof of ultimate limit state as well as serviceability limit states must be provided. Depending on the geometry and load combinations, dimensions will be determined either by the ultimate limit state or the serviceability limit state. As the values in Table 7 show, the serviceability limit state is critical for all slabs. The explanation lies in the minimum strength of the carbon mesh-reinforced shotcrete layer and the therefore minimal increase in stiffness. It can hence be deducted that there is limited possibility for reinforcement using the S&P ARMO-system on constructions that have already reached their serviceability limit state.

5.1.2 Structural Behaviour at the Ultimate Limit State

Onset of plasticity in the Reinforcing Steel

The structural behavior of the test slabs changes dramatically when the reinforcing steel begins to yield. When the reinforcing steel's strain surpasses the yield strain, then the additional internal tensile forces must be borne primarily by the carbon mesh. The reinforcing steels only carry loads in relation to the strain hardening modulus, whose value lies below 1% of the elastic stiffness – the reinforcing steels therefore hardly carry any load as compared to the carbon meshes. The reinforcing steel's yielding thus marks the beginning of the carbon meshes' actual load load-bearing behavior. The resulting forces and deflections at mid-span can be estimated from the load-deflection curves.

The comparisons listed in Table 7 show that the yield loads and the respective deflections at mid-span increase only a limited degree with larger carbon mesh cross-sections. Certain deviations can be ascribed to reading inaccuracies. However, the general tendency is for the yield loads to increase with stronger carbon mesh reinforcement. The carbon meshes' stiffness is thus somewhat activated even before the reinforcing steel begin to yields though not to its full capacity. The larger yield loads with increasing carbon mesh cross-section also prove, that at the cracked state, the bond effect between the carbon mesh and the spray mortar surrounding may be small but not negligible.

Based on the increase in deflection $w_u - w_y$ from the point of the reinforcing steels' yielding at Q_y up the ultimate load Q_u reduction factor can be determined for the flexural stiffness EI_y at the plastic state of the reinforcing steel with respect to the stiffness at the cracked but still elastic state EI_{II} (Table 6). This can be compared to the deflection increase for the working loads (from 8 kN to 16 kN, also refer to Table 7).

This clearly shows the influence of the carbon meshes' strain stiffness. In contrast to the expected reduction of the flexural stiffness, given the present degree of reinforcement, by a further factor of roughly 8 as compared to an unreinforced concrete girder, the reduction for Test Slab D1 is roughly below 2. For Test Slab D2 the stiffness is reduced by only about 25 %.

This very favorable influence of the carbon meshes is confirmed in the increased ratios Q_u/Q_y (yield load to ultimate load measured) of roughly 30 % per layer of carbon mesh.

	Q_y [kN]		W_y [mm]	EI_y/EI_{II}	Q_u [kN]		w_u [mm]	Q_u/Q_y	Q_{rest} [kN]		$w_{remainder}$ [mm]	$D_s = w_u/w_y$	
D0	38.7	100%	61	7.98	47.2	100%	176.5	122%	--	--	--	2.89	100%
D1	42.1	109%	62	1.95	63.8	135%	141.7	152%	52.4	82%	162.8	2.29	79%
D2	44.4	115%	58	1.34	80.0	170%	132.7	180%	56.2	70%	155.1	2.29	79%

Table 7: Characteristic values of the ultimate state and the yield state of the reinforcing steels

Degrees of Strengthening

Based on the ratios of the ultimate loads Q_u of the reinforced slabs, the degree of strengthening by carbon mesh can be determined in comparison to the reference slab (Table 9). The values show that a doubling of the carbon mesh's cross section also results in a doubling of the additional load that can be borne until failure. For the tested structural system, this results in a load increase of about 16.5 kN or 35 % per layer of carbon mesh.

### Crack Patterns and Strains in the Tensile Zone

Graph 10 shows the crack patterns of all test girders at failure as well as the maximum load and the measured strain along the tensile edge.

The crack patters show a sufficiently fine distribution of the cracks for all experiments. For Reference Test D0, the crack spacing corresponds roughly to the distance of the lateral reinforcement, as expected. For Test D1 and D2 with spray mortar strengthening, the tendency is for the crack spacing to be somewhat reduced. This is also to be expected due to the slight stiffening effect of the strengthening. This stiffening effect is also confirmed by the strains at maximum loading, as these decrease with increasing strengthening (Graph 9 / 10).

Failure Behavior and Residual Resistance

Definitive failure principally occurs for all test slabs as compressive failure in the concrete compression zone. None of the slabs fail because the reinforcement steel is pulled apart. Both the bond between spray mortar layer and concrete surface as well as the carbon mesh cross-sections remained intact for both of the strengthened slabs when failure occurred in the bending compression zone.

The load elongation diagram (Graph 10) shows the measured strain on the concrete tension side. The elongation in the *S&P ARMO-mesh* was not measured.
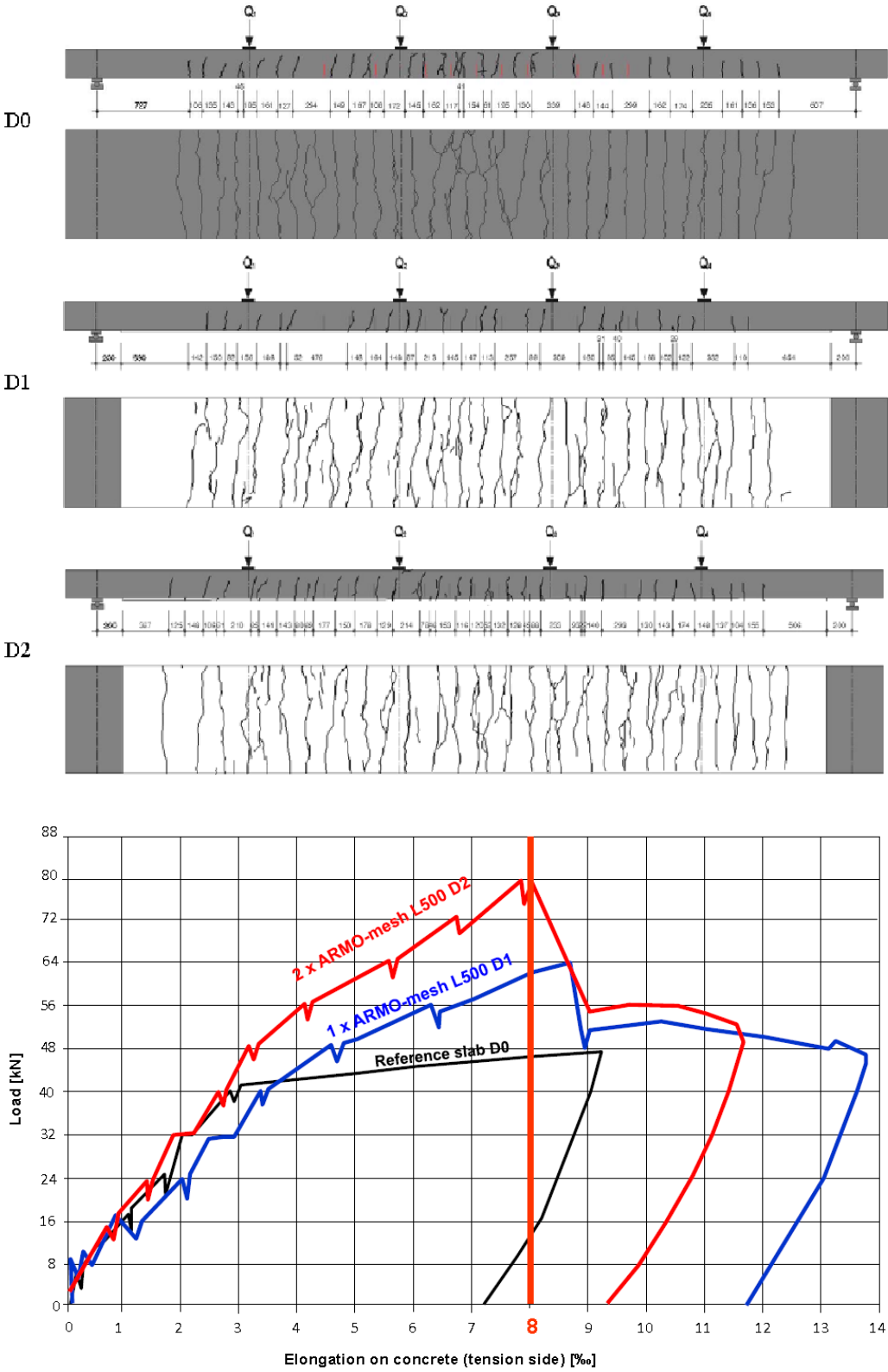
Graph 10: Crack patterns and load/elongation diagram

The maximum elongation on the concrete (tension side) of 0.8 % was used to calculate the theoretical elongation and stress in the *S&P ARMO-mesh*. The results clearly showed that there is a certain elongation required to activate the *S&P ARMO-mesh*. Therefore, in the S&P design concept, the theoretical modulus of elasticity is reduced by a factor 1.5 on one side. On the other side, the ultimate limit strain in the *S&P ARMO-mesh* in flexural enhancement is determined to be 0.5 %. The ultimate limit strain in axial enhancement is determined to be 0.4 %, respectively in shear enhancement to be 0.2 %.

Elastic modulus (theoretic) of S&P ARMO-mesh	**240 kN/mm^2**
Reduction factor for the elastic modulus of S&P ARMO-mesh	**1.5**
Elastic modulus (reduced) of S&P ARMO-mesh for design	**160 kN/mm^2**

Ultimate limit strains of S&P ARMO-mesh:

Flexural tension	**0.5%**	**(~ 800 N/mm^2)**
Axial	**0.4%**	**(~ 650 N/mm^2)**

6. *S&P ARMO-flexion* Software for flexural tension strengthening

S&P ARMO-flexion (Figure 11) serves as design software for the strengthening of reinforced and prestressed concrete structural elements subject to uniaxial bending combined with axial force using the *S&P ARMO-System*. The program can be used both for the design of strengthening measures as well as to produce verifiable check calculations as part of a structural analysis. The program yields the necessary carbon fibre cross-section for S&P *ARMO-mesh L500, L200 or 200/200*. In addition, the software performs anchorage checks as required by the S&P ARMO-System design guidelines. Tested standardized spray mortars *S&P ARMO-crete d* and *S&P ARMO-crete w* are used. The design follows the technical approvals as well as recommendations and codes for adhesive reinforcing and FRP reinforcements. A design example is available in the appendix.
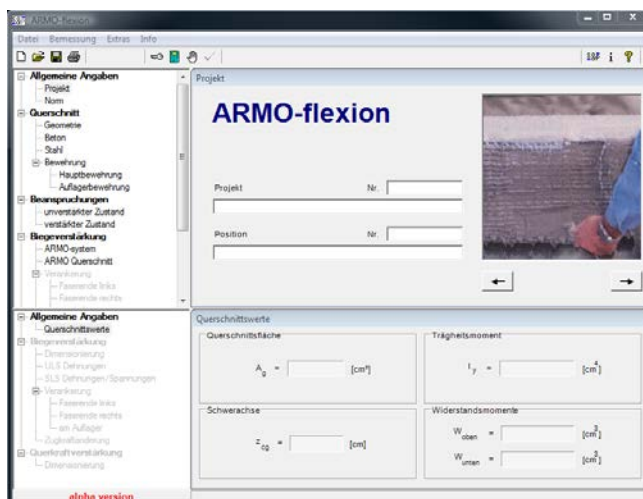

Figure 11: ARMO-flexion design software

7. *S&P ARMO-axial* Software for Axial Strengthening

S&P ARMO-axial (Figure 12) is design software for the strengthening of axially compressed reinforced concrete columns using the *S&P ARMO-System*. Strengthening is based on the fact that wrapping the column prevents lateral/radial expansion of the column. This creates a triaxial stress state in the concrete, which increases the concrete compressive strength.

S&P

S&P ARMO-axial can be used both for the design of strengthening measures as well as to produce verifiable check calculations as part of a structural analysis. For a pre-defined load, the program will calculate the necessary number of wrapping layers of *S&P ARMO-mesh L500 or L200*. Tested standardized spray mortars *S&P ARMO-crete d* and *S&P ARMO-crete w* are used. The design follows the technical approvals as well as recommendations and codes for adhesive reinforcing and FRP reinforcements. A design example is available in the appendix.
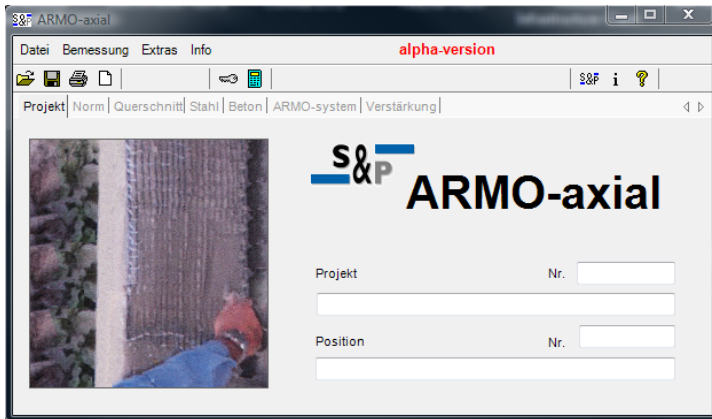

Figure 12: ARMO-axial design software

8.   FRCM Applications in Tunnels and General Civil Works

Shotcrete is used in tunnel construction in order to secure excavations or for the actual tunnel lining. When securing excavations the shotcrete is primarily reinforced using steel fibres. Laying reinforcement mats in an unsecured excavation is too problematic due to safety concerns. For shotcrete tunnel linings, steel reinforcement mats are generally used. Especially in conventional tunnel excavation, the unevenness of the tunnel surface is very pronounced. Steel mats can thus not be placed in a way that tightly follows the tunnel vault. Additional shotcrete is necessary to even out the surface.

> **When using *S&P ARMO-mesh,* the shotcrete layer is thinner. The flexible carbon mesh and thus the shotcrete lining follow the unevenness of the tunnel profile or the excavation pit.**

When the bearing surfaces are uneven, the steel reinforcing is relatively distant from that bearing surface over large areas. During the shotcreting process, the steel mats begin to vibrate resulting in increased recoil and the creation of a spray voids behind the reinforcement (Figure 13).

Figure 13: Spray voids behind steel reinforcing

Figure 14: Fixing of S&P mesh using clamps

Advantages of the *S&P ARMO-System*:

- The shotcrete layer's thickness can be reduced (less need to even out the profile / less cover for the carbon fiber reinforcement).
- The carbon fiber is inert and thus not subject to corrosion. Aggressive mountain water or alternating current cannot harm the reinforcement in the long run.
- The pH-value of the shotcrete is irrelevant to the corrosion protection of the reinforcement. Carbonation of the concrete, e.g. in vehicular tunnels, does not impact the functioning of the carbon reinforcement. Chlorides which may penetrate into the shotcrete around the portals do not cause damage to the carbon mesh either.
- A later widening of the tunnel (pilot drift) is also possible without problems. The carbon mesh does not adversely affect subsequent milling operations.

For general civil works there are various possibilities for application. Figures 15 and 16 show a shotcrete wall. The shotcrete was tempered with steel fibers. The *S&P ARMO-mesh 200/200* was applied locally around the anchorage points. Additionally, strips of *S&P ARMO-mesh L500* were laid across the anchor heads and sprayed over. The *S&P ARMO-mesh* was fastened using an S&P rotary disk.
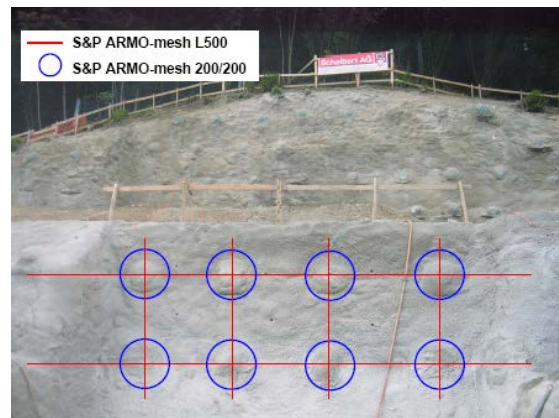
Figures 15 / 16: Local strengthening at anchor heads

Comparison of shotcrete lining with steel reinforcement / *S&P ARMO-mesh*

The criterion for comparison of reinforced shotcrete linings is the work capacity as defined in SIA 162/6 (test dated 1999).

A 10 cm thick shotcrete layer with a reinforcing layer 150/150 Ø 6 (K188) placed in the middle usually has a work capacity of around 800 Joules. This work capacity can also be achieved with about 25 - 30 kg/m^3 of steel fibres. At the test drift in Hagerbach, Switzerland, (P 10 / P 19) the work capacity of a 10 cm thick shotcrete lining with *S&P ARMO-mesh* was tested.

For the test, an 8 cm thick traditional shotcrete layer was applied. Afterwards, the *S&P ARMO-mesh* was placed into a 2 cm thick layer of *S&P ARMO-crete d*.

Two mesh variants were tested:
- *S&P ARMO-mesh L500* (unidirectional carbon fibre)
- *S&P ARMO-mesh 200/200* (bidirectional carbon fibre)

Figures 17 through 19 shows the application. Table 8 lists the results in comparison to a steel reinforcement mesh 150/150 Ø 6 mm.

Figures 17/18/19: Application of the test specimen to determine work capacity

Test Specimen	Work Capacity
10 cm standard shotcrete with steel reinforcement in center (mesh Ø 6mm 150/150)	800 Joule
8 cm standard shotcrete with single layer of *S&P ARMO-mesh L500* in 2 cm *S&P ARMO-crete d* (anchored)	**1,139 Joule**
8 cm standard shotcrete with single layer of *S&P ARMO-mesh 200/200* in 2 cm *S&P ARMO-crete d*	**824 Joule**

Table 8: Hagerbach Test Drift Results (P10/P19)

The S&P ARMO-System is especially well suited for the rehabilitation and structural strengthening of damaged concrete or shotcrete linings of adits, pressure tunnels or for roads and railways.

> **The prevailing advantage of the S&P ARMO-System consists of the thinner shotcrete layer necessary (by several centimeters) so that the discharge capacity or clear interior profile available after rehabilitation is greater.**

S&P

Reinforcing steel meshes installed in a shotcrete layer require a thickness of about 8 cm for rehabilitations. This minimum layer thickness is necessary in order to equalize any unevenness, embed the reinforcing and provide a 3 cm cover for the steel reinforcement. This 3 cm concrete cover is necessary in order to guarantee sufficient fire resistance (F60) and safeguard the interior reinforcement from corrosion (pH value of 12 inside the shotcrete). The S&P ARMO-mesh only requires a cover of 2 cm to achieve the same fire resistance F60 (refer to Section 10). A minimum cover for corrosion protection is not required. For this reason, the shotcrete layer thickness is reduced by roughly 50 % (refer to Table 9).

	Shotcrete Layer Thickness in cm	
	Conventional steel mesh	*S&P ARMO-System*
Equalizing any unevenness	3	1 – 2
Embedding	1 - 2	irrelevant
Cover	3	1 – 2
Total	**7 - 8**	**2 – 4**

Table 9: Thickness reduction for the shotcrete layer

For the rehabilitation e.g. of a headrace tunnel of a hydroelectric power plant most often oven-dried shotcrete is used for logistical reasons (in sacks or in bulk). S&P offers prefabricated shotcrete for pneumatically actuated guniting. The spray mortar *S&P ARMO-crete d* (dry) is produced in varying grains and with various additives and cement types. The delivery of the silo stock or bagged materials is possible from various production locations.

The following shows a cost comparison for 8 cm traditional shotcrete with reinforcement layer and a 4 cm thick shotcrete lining using the *S&P ARMO-System*.

8 cm traditional shotcrete lining with steel reinforcement layer

Material costs, bagged shotcrete, 8 cm à ca. €6-8.--/cm	€ 56.--/m^2
Application costs	€ 17.--/m^2
Delivery and application of steel reinforcement (difficult conditions)	€ 25.--/m^2
Total	**€ 98.--/m^2**

4 cm *S&P ARMO-crete d* with S&P ARMO-mesh L500 or 200/200

Material costs for S&P ARMO-crete, 4 cm à ca. €8-9.--/cm (+30%)	€ 34.--/m^2
Application costs (+ 25 % as the amount sprayed is smaller)	€ 20.--/m^2
Delivery and application of S&P ARMO-mesh	€ 22.--/m^2
Total	**€ 76.--/m^2** (-20%)

The *S&P ARMO-System* has the following additional advantages for the client:
- The ARMO-mesh replaces the steel reinforcement; the shotcrete layer is thinner.
- No spray shadow/void behind the *S&P ARMO-mesh*.
- Less recoil, since there is no vibration as would occur with steel reinforcement.
- 3 x higher heat resistance and only 1 cm of concrete cover necessary for R60.
- No corrosion of the carbon reinforcement and minimum required concrete cover.
- Greater clear interior profile or discharge area for the tunnel.

9. Seismic Strengthening of Masonry – Comparison FRP / FRCM
9.1 Strengthening using FRP Systems

In the years 2007/2008, 15 masonry walls were cyclically loaded at the FH Fribourg (CH). The masonry was reinforced using different S&P FRP systems (strips, sheets, etc). The FRP reinforcement was always anchored in the adjacent concrete areas. Figure 20 and Graph 11 show the test arrangement.

Figure 20: Test rig at FH Fribourg
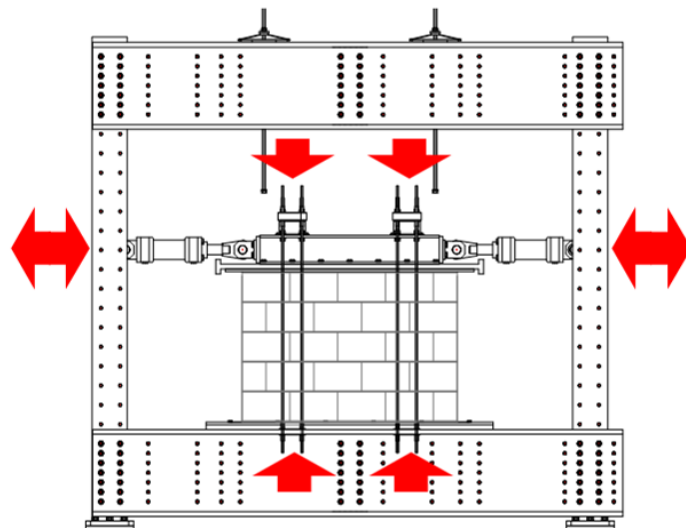
Graph 11: Test arrangement at FH Fribourg

Two different series were run.
Series A   Vertical load of 1.0 N/mm^2 [P16]
Series B   Vertical load of 0.5 N/mm^2 [P17]

A very high load was chosen for Series A. As the vertical load is reduced in a seismic event (vertical lift-off of the element) the load was reduced in Series B. Table 10 lists the results obtained for Series B. The masonry was reinforced with *S&P C-Sheet 240* of 200 g/m^2 (bands of 300 mm width) in different arrangements on one or both sides (Figures 21 through 23).

		Horizontal load %	Horizontal deflection %
B1:	Reference	100	100
B2:	2 vertical bands	118	105
B3:	2 vertical bands + 2 bands at 45º	149	110
B4:	4 vertical bands + 45º	170	107
B5:	2 vertical bands + 60º	167	102

Table 10: Result summary for S&P C-Sheet 240, 200 g/m^2 in different arrangements
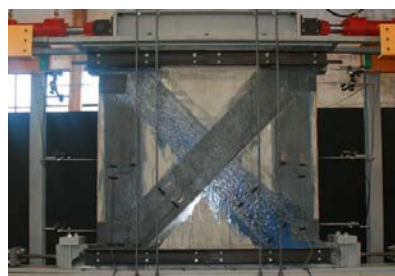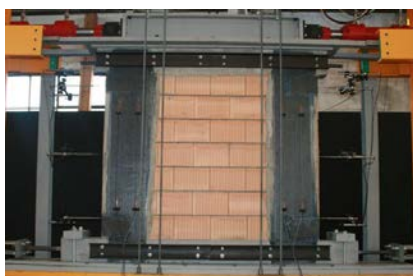
Figures 21 / 22 / 23: Different arrangements of the S&P C-Sheet 240

Deductions:

The results of the cyclic load tests show that FRP-reinforced walls can resist significantly higher horizontal loads than unreinforced walls. The reinforcements on one or both sides showed comparable results. However, the increased resistance of the reinforced masonry walls can only be utilized comprehensively if the bricks and joints can resist the increased loads. The deflections of the reinforced masonry walls were generally increased by up to 10 %. It should therefore be possible to reinforce load-bearing masonry walls of existing structures especially in zones with a lower risk of seismic activity and for such structures that fall into building categories I or II.

9.2   Strengthening using FRCM System

In order to investigate the behaviour of the *S&P ARMO-mesh,* another test series C [P18] was performed at FH Fribourg. These identical tests were executed this time using the *S&P ARMO-mesh L500* (200 g/m^2) instead of the FRP system *S&P C-Sheet 240* (200 g/m^2). An identical width and fiber amount for the reinforcement bands was chosen.

The *S&P ARMO-System* was anchored in the adjoining concrete element and applied on one side only. Figures 24 and 25 show the application of the *S&P ARMO-System*.

Figures 24 / 25: Application of the S&P ARMO-System

S&P ARMO-mur, a plaster with reactive component, was used as spray mortar. The plaster can be applied by hand or mechanically. The vertical load in Series C is identical to the load used in Series B.

Table 11 lists the results for Series C, where the *S&P ARMO-System* was used as reinforcement. The comparative values for Series B (*S&P C-Sheet 240*) are given in Table 11 as well.

	Horizontal load %	Horizontal deflection %
C1: Reference	100	100
C2: 2 vertical bands	145 *118 (B2)*	138 *105 (B2)*
C3: 2 vertical bands + 2 bands at 45º	147 *149 (B3)*	111 *110 (B3)*
C4: 4 vertical bands + 45º	159 *170 (B4)*	119 *107 (B4)*
C5: 2 vertical bands + 60º	161 *167 (B5)*	108 *102 (B5)*

Table 11: Result overview for S&P ARMO-System in different arrangements / Comparison

> **The strengthening effect of the S&P FRCM System is comparable to the results for the FRP strengthening.**

For all tests regarding the "seismic reinforcing of masonry" using S&P products, the reinforcement bands were always anchored in the adjacent structural member. In practice, this is possible using the S&P Anchorage Element Alu (Graph 12). Figures 26 through 28 show an on-site application for seismic strengthening of a masonry wall and end anchorage using an *S&P ARMO-mesh.*
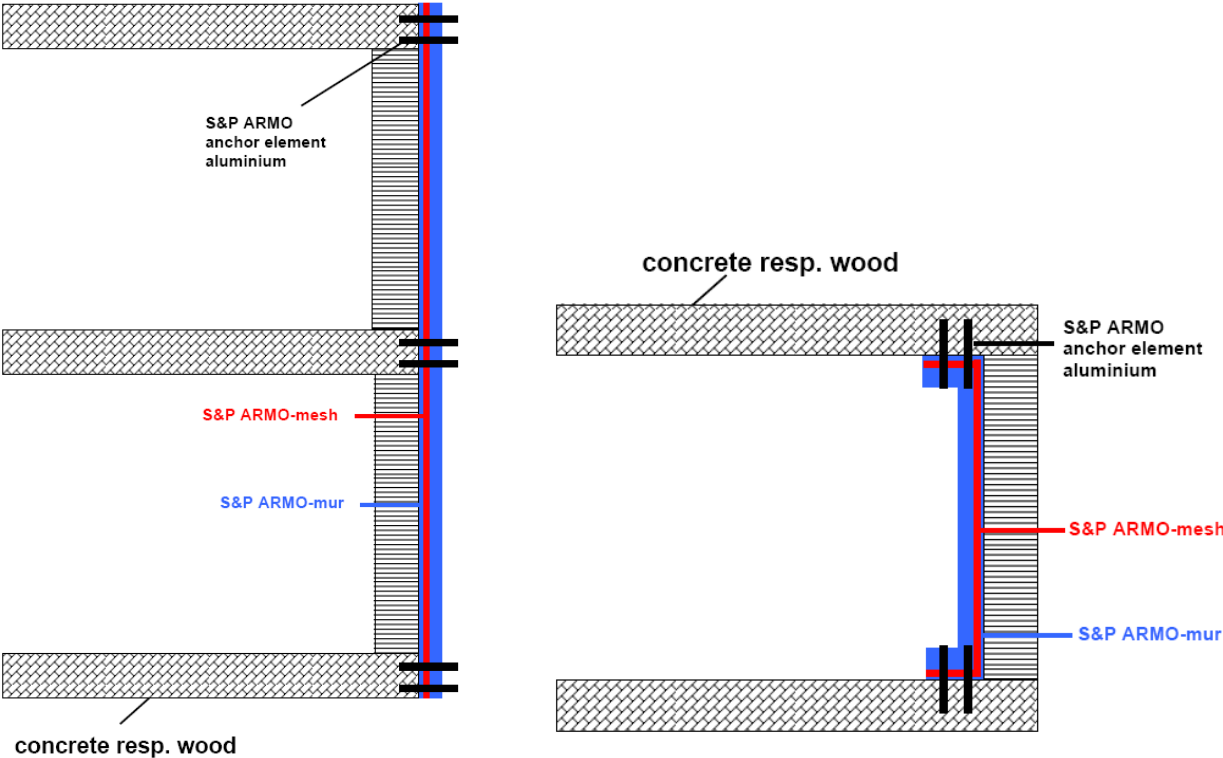
Graph 12: Connection details of adjacent member

> **In this case, the tensile force is fully anchored through the dowels connecting with the adjacent concrete member.**

Figures 26 / 27 / 28: seismic strengthening and anchorage of a masonry wall using S&P ARMO-mesh

Reinforcing masonry walls using carbon-fibre ARMO-mesh embedded in spray mortar is a new, cost-effective and innovative technology.

10. Fire Tests with S&P FRCM System at EMPA Dübendorf/CH and Hagerbach VSH/CH Testing Tunnel

According to DIN 4102 (Section 5.2.7) the steel temperature in case of fire must not exceed the critical temperature of 500 °C. In ASTM, E119-12 (Section 8.7.6.3) [N3], the critical temperature is 427 °C. While the tests are not performed under working loads in Germany, the US and various other countries require tests under working loading. S&P performed fire tests for the *S&P ARMO-System* at the EMPA Dübendorf/CH and in the Hagerbach VSH/CH Testing Tunnel.

10.1 Tests at EMPA Dübendorf/CH

At EMPA/CH, the critical temperature of the S&P carbon mesh was investigated [P24]. From the *S&P ARMO-mesh L500,* the carbon rovings were cut out in the longitudinal direction. These were then tested under axial tension after having been subjected to high temperatures for 30 minutes. Figure 29 shows the cylinder oven.

Figure 29: Cylinder oven

The total length of the carbon specimens was roughly 1.6 m. Only the middle part of roughly 40 cm in length was subjected to heat in the cylinder oven. The ends of the carbon rovings were kept outside the oven at room temperature.
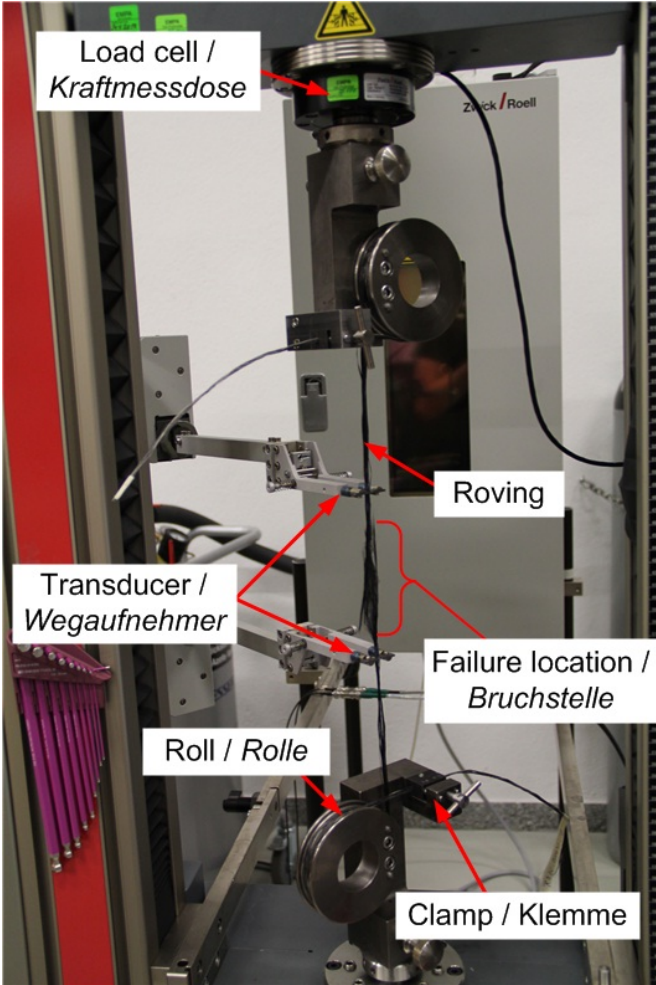

Figure 30: Test arrangement

Figure 30 shows the test arrangement. The carbon rovings were reeled up at either end three times and clamped into the tensioning apparatus. The tensile force was applied by controlling the path with a speed of 5 mm/min.
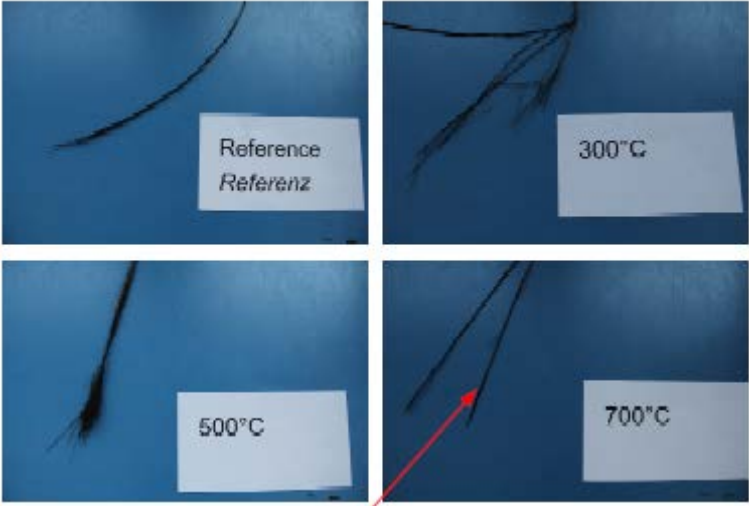

Figure 31: Specimens after the tests

Figure 31 shows the specimens after the tests as well as the point of failure (red arrow). The heat affects the coating of the carbon rovings. The tension test required an additional prestrain. The heat was applied for 30 minutes at temperatures of 300, 500, 700 and 1000 °C. Aside from the heat-treated specimens, a reference roving was also tested.
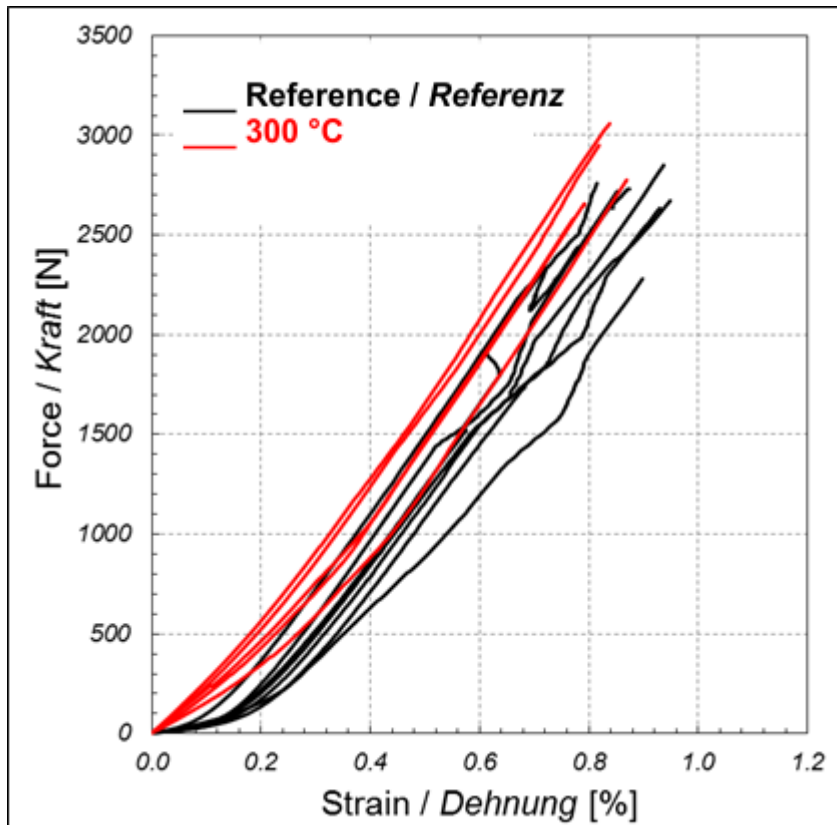
Graph 13: Stress/strain curve

The stress/strain curve (Graph 13) shows the reference roving in comparison to the roving which was heated up at 300 °C. While the tensile elastic modulus is not reduced, the reduction in tensile strength is clearly visible (Table 12 / Graph 14).

|	Reference (Force N)	300°C	500°C	700°C	1000°C
1	2731	2776	998	72	46
2	2281	3058	1930	66	36
3	2760	2657	1516	55	23
4	2672	2949	1729	45	50
5	2635	2582	1541		
6	2719				
7	2850				
Average	**2664**	**2805**	1542	**60**	**39**
s.d.	182	198	347	12	12
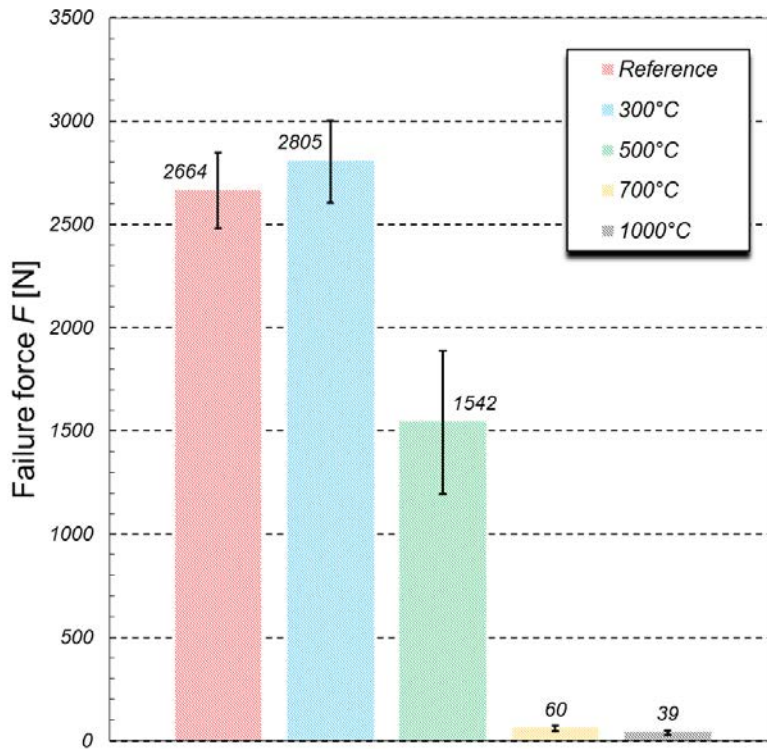
Table 12 / Graph 14: Average values of the maximum tensile strength

Results / Summary of Tests at EMPA/CH

The tests at EMPA/CH clearly show that 30 minute heat application at 300 °C causes a slight increase of roughly 5% in average maximum tensile strength (increase from 2664 to 2805 N). Due to the additional prestrain of the heated rovings, the failure strain is roughly the same for all series. The stiffness (tensile elastic modulus) is thus quasi identical for the reference roving and the heated rovings. An increase of the temperature to 500 °C causes an average strength reduction in comparison to the reference tests by 1122 N, equivalent to a loss in strength of 43%. As the S&P ARMO-mesh is utilized at roughly 20% of the carbon roving's theoretical failure load (800 N/mm^2) this strength loss in the case of fire is not decisive. For this reason, the manufacturer recommends to use 500 °C as the critical temperature for the S&P ARMO-mesh.

10.2   Fire Tests at the Hagerbach VSH/CH Testing Tunnel

In order to provide strong fire resistance e.g. in tunnel construction, fire protection mortars with special aggregates (vermiculite or others) as well as special cements are available. These products resist fires only if the structural concrete below can resist the fire loading as well. Figure 32 shows spalling of a structural surface that was protected by such special mortar. In order to prevent spalling in fire tests, the structural surface can be improved by e.g. polypropylene (PP) fibers. Figure 33 shows the impeccable surface of the specialized product after a fire test on a concrete surface containing PP fibers. Such results can be misleading. Only in the rarest of cases do concrete structures that require fire protection have surfaces containing PP fibers.

Figure 32: Spalling of a structural concrete surface

Figure 33: No spalling of the structural surface occurred as the concrete was laced with PP fibers

> **Therefore, it is important that the designer chooses the proper structural surface and fire curve, based on the actual conditions of the object to be protected.**

At the Hagerbach VSH/CH Testing Tunnel, the fire test was performed on a concrete slab that was strengthened using the ARMO System. The ARMO System uses common aggregates and typical Portland cement. According to the various European codes, different fire curves (refer to Graph 15) are available depending on the application, i.e. whether it is a building, other structure, or a tunnel.
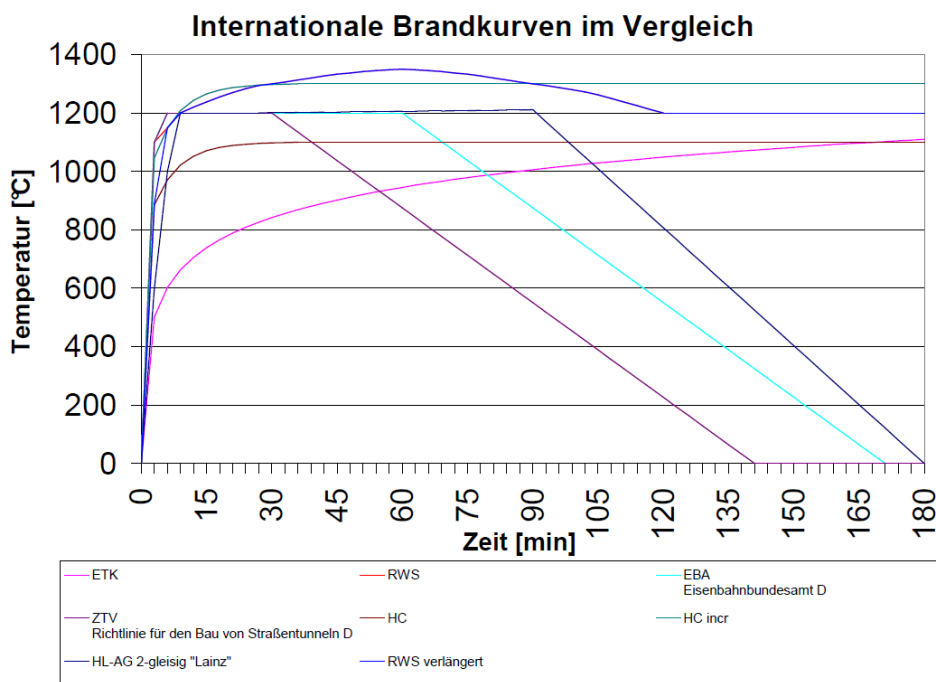
Graph 15: Comparison of international fire curves

The test in the Hagerbach tunnel was performed in accordance with the standard fire curve (ETK) and RWS. The standard curve is used in Europe for buildings and other general structures. The fire loading in the testing tunnel using the standard curve was applied for 120 minutes. The RWS curve is usually applied in The Netherlands for tunnel structures below sea level. The fire loading in the testing tunnel according to RWS was applied for 60 minutes. In the test specimen the residual humidity was limited to 4%.

Test Arrangement

A reinforced concrete slab with a 2.0 m span, a width of 0.95 and a thickness of 0.2 m was produced. The existing interior steel reinforcement (5 bars Ø 8 mm) was covered by a 3 cm layer of concrete. Afterwards, 2 cm of this layer were removed hydromechanically. The remaining concrete cover of the reinforcing steel was thus 1 cm. Then the S&P ARMO-system was applied as follows,

- 1 cm ARMO-crete w of wet spray mortar was applied
- 2 layers of ARMO-mesh 200/200 were inserted in the first spray mortar layer
- 2 cm cover of wet spray mortar was applied over the ARMO-mesh layers

Thus:

| Reinforcement cover:	- steel reinforcement	4 cm in total
	- carbon reinforcement	2 cm in total

The fire test was performed under working loading (Figures 34 / 35):

Figure 34 / 35: Working load during testing

Two concentrated loads of 24 kN were applied as working loads. The failure moment at the limit state (self-weight of the slab and concentrated loads) was 27.2 kNm. The corresponding bending moment under working loads was then 18.3 kNm. The stresses and strains of the reinforced slab at the failure and serviceability were determined with the ARMO-flexion design software and are shown in the following:

strains - ultimate limit state ($A_{f,req}$)

$$\varepsilon_c = -0.812 \ [‰]$$
$$x = 2.7 \ [cm]$$

$$\varepsilon_s = 3.693 \ [‰]$$
➡ $$\varepsilon_f = 4.5 \ [‰]$$
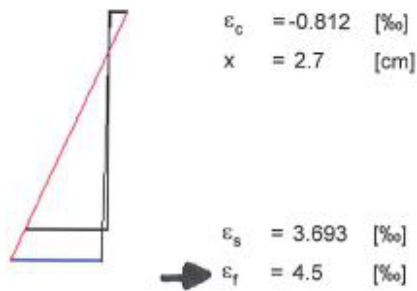
strains / stresses - service limit state ($A_{f,prov}$)

$$\varepsilon_c = -0.344 \ [‰]$$
$$x = 2.85 \ [cm]$$

$$\varepsilon_s = 1.466 \ [‰] \qquad \varepsilon_{sy} = 2.5 \ [‰] \quad \checkmark$$
➡ $$\varepsilon_f = 1.6 \ [‰]$$
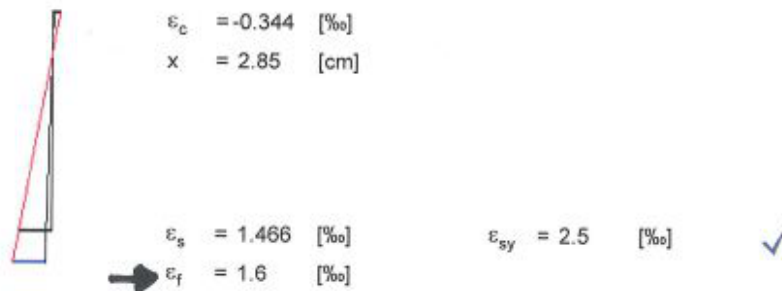
stresses   stress limits

concrete	$\sigma_{c,max} = -9.44$	[N/mm²]	$\sigma_{c,limit} = -18$	[N/mm²]	
reinforcing steel	$\sigma_{s,max} = 293.26$	[N/mm²]	$\sigma_{s,limit} = 400$	[N/mm²]	$\checkmark$
carbon fibres ➡	$\sigma_{f,max} = 383.95$	[N/mm²]			

Graph 16 shows the distribution of the temperatures in the steel and carbon reinforcement over time.
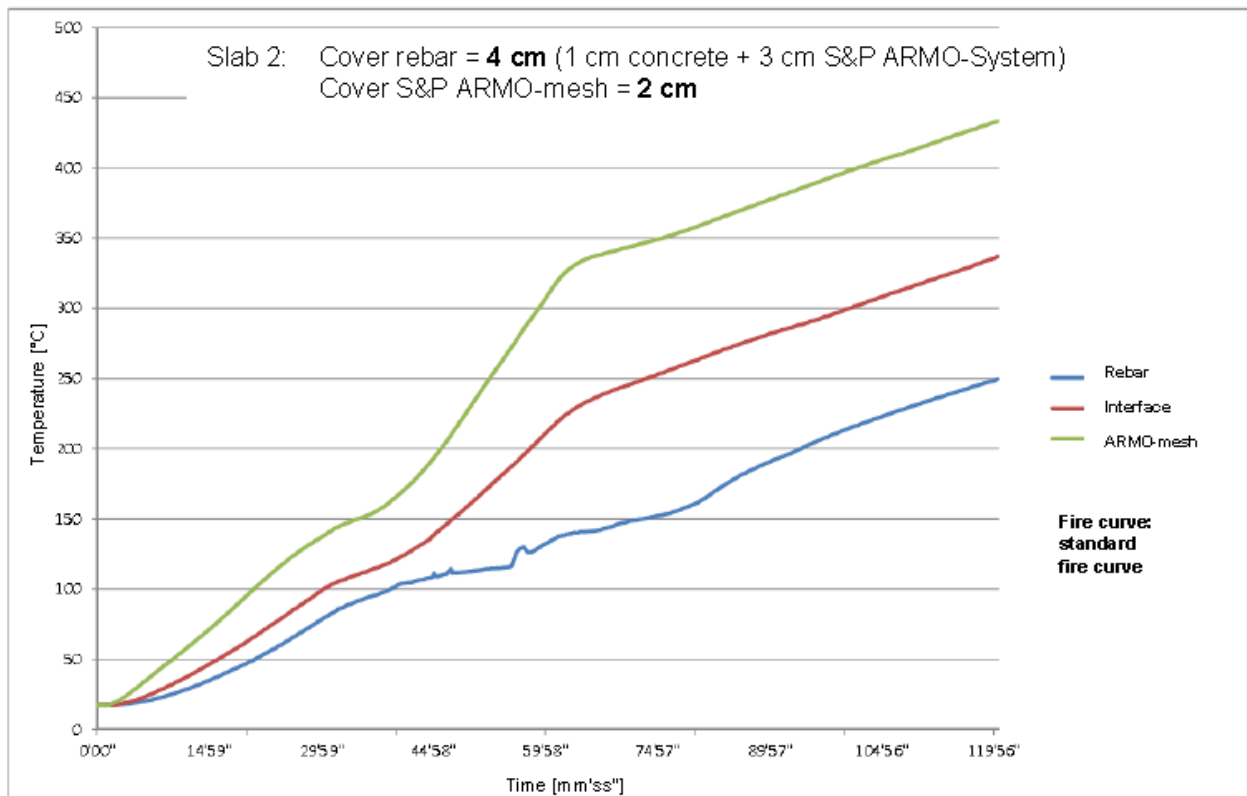
Graph 16: Results of the standard fire curve tests at Hagerbach Testing Tunnel/CH
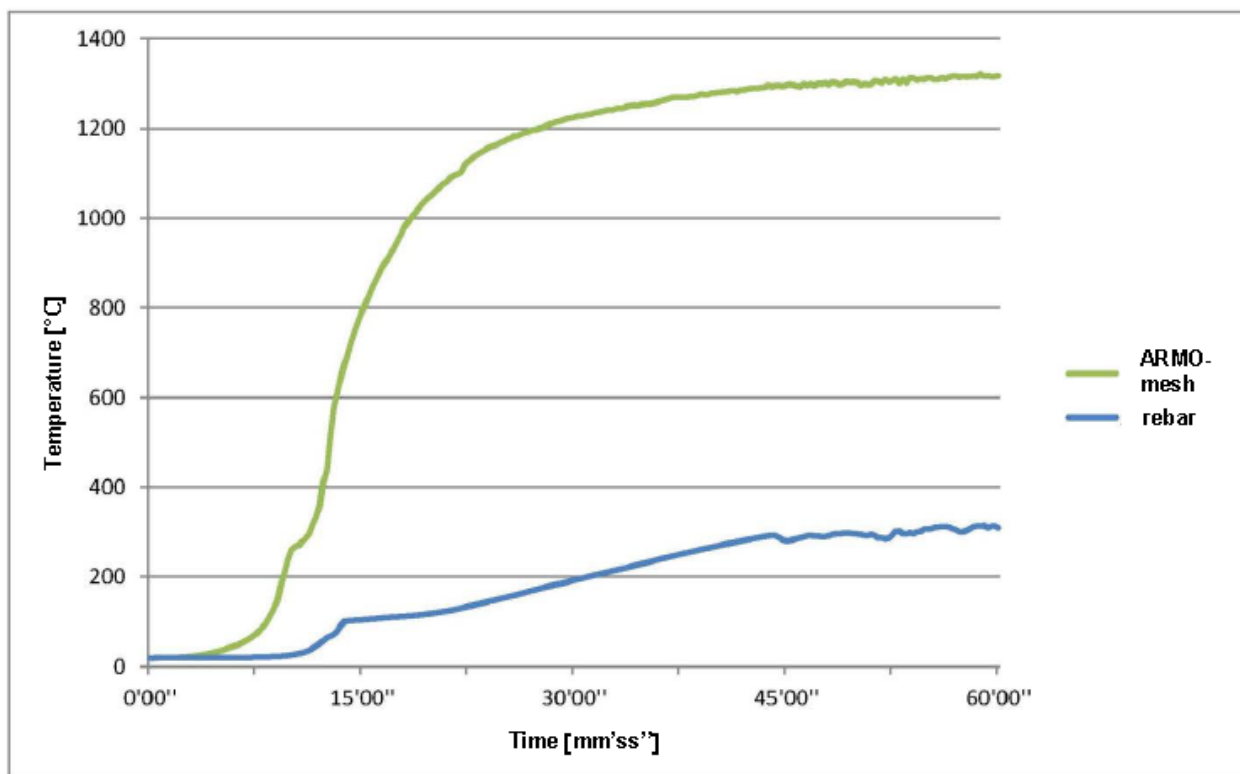
Graph 17: Results of the fire tests using the RWS curve at Hagerbach Testing Tunnel/CH

Results:

After 120 minutes of standard curve fire loading under working loads, the temperature in the S&P ARMO-mesh (mat) reached 440 °C and 250 °C in the reinforcement steel. The critical temperature was not reached, neither in the carbon mesh nor in the reinforcement steel.

After 60 minutes of RWS curve fire loading under working loads the temperature in the S&P ARMO-mesh (mat) reached 1300 °C and 300°C in the reinforcement steel. The critical temperature of 500 °C(DIN) was not reached in the reinforcement steel.

10.3 Evaluation of the Fire Tests

Analogous to the FRP strengthening, there are two possible evaluation cases:

Case 1:
For a low degree of reinforcement using S&P ARMO-system, the residual safety against failure of the ARMO reinforcing is > 1.2. In this case, the ARMO system is applied on one hand in order to increase the safety level at the ULS, but also as fire protection for the internal steel reinforcement. For the evaluation under fire loading, the critical temperature of the steel reinforcement is the governing factor.

Case 2:
For a high degree of reinforcement using S&P ARMO-system, the residual safety against failure of the ARMO reinforcement is < 1.2. In this case, the ARMO-system is applied in order to increase the safety level at the ULS. For the evaluation under fire loading, the critical temperature of the carbon mesh (S&P ARMO-mesh) is therefore the governing factor.

11.   S&P ARMO-mesh Quality Control

For controlling the quality of textile reinforcement, the tensile test of wide strips according to EN ISO 10319 is often applied. Generally, this test is not suitable for brittle materials such as carbon fibers. As the carbon fiber used in the S&P ARMO-mesh is coated using an amorphous silica layer, there are fine grains present in between the clamp and the carbon roving. This results in punctual loading of the filaments near the roving's surface. The roving then fails early. Quality control on the final, coated S&P ARMO-mesh is therefore not possible according to EN ISO 10319. The quality of S&P ARMO mesh is thus controlled on the impregnated carbon strand. The carbon strand in longitudinal or lateral direction consists of one or two rovings depending on the how the mesh is produced. Due to the impregnation of the strand with epoxy, the load transfer between the individual carbon filaments within a strand is guaranteed. The clamping area for the tensile test must be modified specifically to ensure that a continuous pressure is exerted on the carbon strand along the entire length of the clamp (Figure 36). In Test Report No. 461'199 [P26] of EMPA/CH the following average tensile forces were determined:

|	
Fiber strand composed of 1 x 1600 tex	**2759 N**
Fiber strand composed of 2 x 1600 tex	**4938 N**
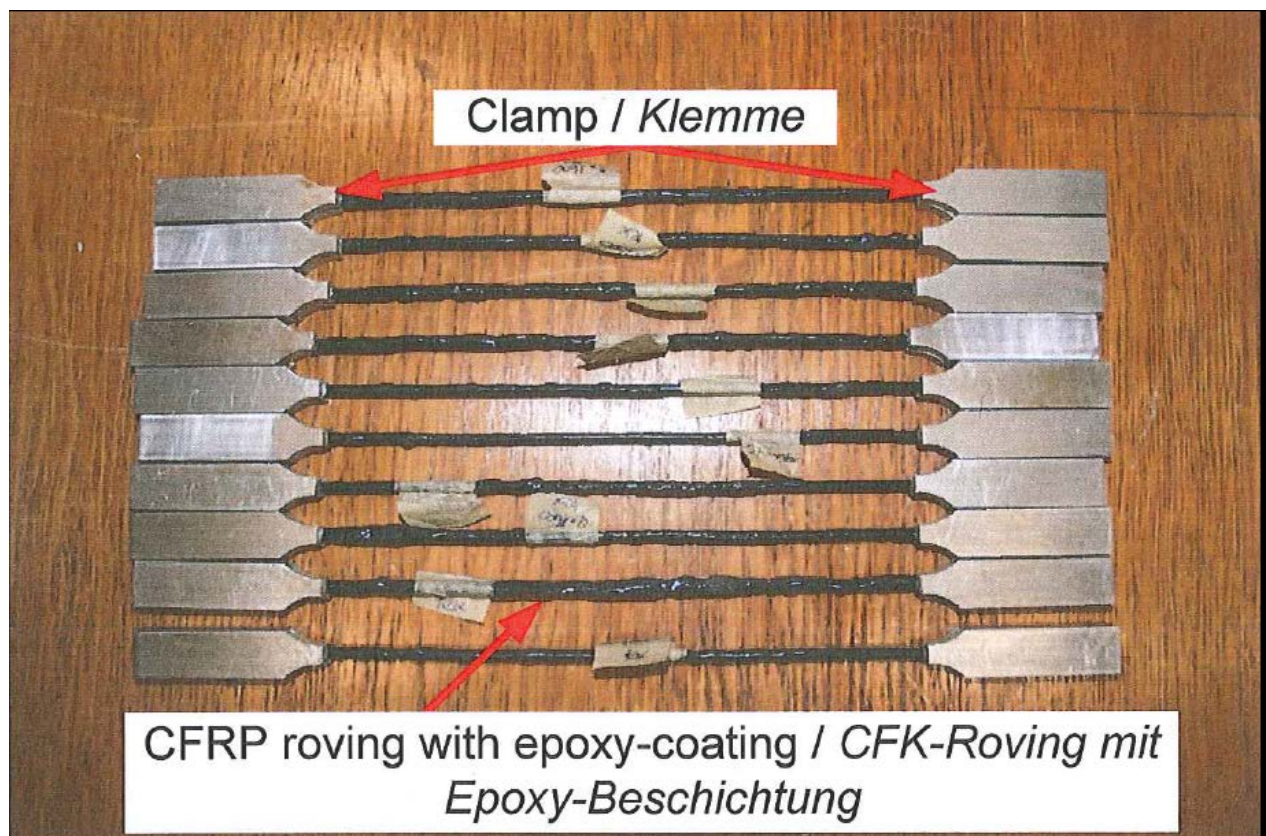
Figure 36: Fiber strands of S&P ARMO-mesh with epoxy-coated clamp detail

Table 13 lists the results of the tensile tests performed at EMPA/CH in comparison to the theoretical characteristic values of the S&P ARMO-mesh L500.

S&P ARMO-mesh L500	Tension / strand (2 rovings/strand)	Tension / m (58.5 strands/m)	Comparison %
Theoretical tensile strength of the C fiber	**7179 N**	**450 kN/m**	**100 %**
Tensile force at the epoxy-impregnated semi-completed product at EMPA/CH	**4938 N**	**288 kN/m** (58.5 x 4937.8 N)	**64 %**
Tensile force at room temperature of the final product with silica coating at EMPA/CH	**2664 N** (Section 10.1 Table 12)	**155 kN/m**	**34 %**
Tensile force at 500°C of the final product with silica coating at EMPA/CH	**1542 N** (Section 10.1 Table 12)	**90 kN/m**	**20 %**
Design tensile force (at ULS 800N/mm²)	**1435 N**	**84 kN/m**	**19 %**
Design tensile force (at ULS ~ 450 N/mm²)	**807 N**	**47 kN/m**	**10 %**

Table 13: Comparison of tensile forces for the S&P ARMO-mesh

It should finally be noted that in actual application of the S&P ARMO-System, the load transfer occurs along the entire fiber length and therefore no problems occur in the clamping area. Taking this into consideration, it becomes clear that for silica-coated rovings there are sufficient reserves at the failure state.

12.   Test Reports/References [P] – Standard Notes [N]

S&P In-house Versuch

P11   Endverankerungen von S&P ARMO-mesh L500, Okt. - Dez. 2009,
       S&P Clever Reinforcement Company AG/CH

Zugversuche / Endverankerung FH Fribourg/CH

P23   Power Point Präsentation Prof. René Suter, FH Fribourg/CH

Plattenbiegeversuche VSH/CH

P10   Prüfberichte Nr. 20100468A, S&P ARMO-mesh L500 (in eine Richtung, endverankert)
       Plattenbiegeversuch, 09.04.2010, VSH/CH
P19   Prüfbericht Nr. 20101027 S&P ARMO-mesh 200/200
       Plattenbiegeversuch, 07.05.2010, VSH/CH
P20   Prüfbericht Nr. 20093882A, S&P ARMO-mesh L500 (in eine Richtung)
       Plattenbiegeversuch, 09.04.2010, VSH/CH

Brandversuche VSH/CH und EMPA/CH

P22   Prüfberichte Nr. 20120012 / Nr. 20120021 Brandprüfung S&P ARMO-System, VSH/CH
P24   Test Report No. 460'742 / 460'794 Hitzebelastung S&P ARMO-mesh, EMPA/CH

Zugversuche an CFK-Rovingen mit Epoxy-Beschichtung EMPA/CH

P26   Prüfbericht Nr. 461'199

**Biegezugverstärkung schlanker Stahlbetonplatten mit Carbongittern
FH Fribourg/CH**

P15   Renforcement de dalles en beton au moyen de treillis en fibres de carbone (Projet de
       recherche AGP 14'105)
Pub.10 Biegezugverstärkung schlanker Stahlbetonplatten mit Carbongittern
       Prof. Dr. Daia Zwicky, FH Fribourg/CH

Erdbeben-Verstärkung von Mauerwerk mit S&P Systemen FH Fribourg/CH

P16   Projet de recherche AGP 21'159, Série expérimentale MR-A, Essais de cisaillement de murs
       en maçonnerie renforces, janvier 2010, FH Fribourg/CH
P17   Projet de recherche AGP 21'159, Série expérimentale MR-B, Essais de cisaillement de murs
       en maçonnerie renforces, septembre 2010, FH Fribourg/CH
P18   Projet de recherche AGP 21'159, Série expérimentale MR-C, Essais de cisaillement de murs
       en maçonnerie renforces, septembre 2010, FH Fribourg/CH
P21   Projet de recherche AGP 21'159, Série expérimentale MT-A, Essais de traction de murs
       renforces en maçonnerie, octobre 2010, FH Fribourg/CH

N1   SIA 262 (2013) Betonbau, Schweizer Norm SN 505 262, SIA, Zürich
N2   SIA 260 (2013) Grundlagen der Projektierung von Tragwerken, Schweizer Norm SN 505
       260, SIA, Zürich
N3   ASTM E119-12, Standard Test Methods for Fire Tests of Building Construction and
       Materials, American Society for Testing and Materials (ASTM)

S&P